AGU PUBLICATIONS

Geophysical Research Letters

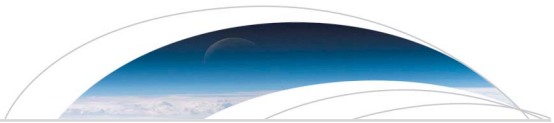

RESEARCH LETTER
10.1002/2017GL072900

**Key Points:**
- The 3-D quasi-simultaneous winds on Venus's day and night from combining space and ground observations
- We detect and quantify day-to-night and temporal wind changes between altitudes 50 and 120 km
- Comparison between wind data and GCM predictions indicates good agreement, but deviations occur at 60–70 km in nighttime

**Supporting Information:**
- Supporting Information S1
- Figure S1
- Figure S2

**Correspondence to:**
J. Peralta,
javier.peralta@ac.jaxa.jp

**Citation:**
Peralta, J., et al. (2017), Venus's winds and temperatures during the MESSENGER's flyby: An approximation to a three-dimensional instantaneous state of the atmosphere, *Geophys. Res. Lett.*, *44*, 3907–3915, doi:10.1002/2017GL072900.

Received 11 DEC 2016
Accepted 30 MAR 2017
Accepted article online 5 APR 2017
Published online 30 APR 2017



# Venus's winds and temperatures during the MESSENGER's flyby: An approximation to a three-dimensional instantaneous state of the atmosphere

**J. Peralta[1], Y. J. Lee[1], R. Hueso[2], R. T. Clancy[3], B. J. Sandor[3], A. Sánchez-Lavega[2], E. Lellouch[4], M. Rengel[5,6], P. Machado[7], M. Omino[8], A. Piccialli[9], T. Imamura[10], T. Horinouchi[11], S. Murakami[1], K. Ogohara[12], D. Luz[7], and D. Peach[13]**

[1]Institute of Space and Astronautical Science (ISAS/JAXA), Kanagawa, Japan, [2]Escuela Técnica Superior de Ingeniería (UPV/EHU), Bilbao, Spain, [3]Space Science Institute, Boulder, Colorado, USA, [4]LESIA, Observatoire de Paris/CNRS/UPMC/Université Paris Diderot, Meudon, France, [5]Max-Planck-Institut für Sonnensystemforschung (MPS/MPEG), Göttingen, Germany, [6]European Space Astronomy Centre, Madrid, Spain, [7]Institute of Astrophysics and Space Sciences, Observatório Astronómico de Lisboa, Lisbon, Portugal, [8]University of Tokyo, Tokyo, Japan, [9]Planetary Aeronomy, Belgian Institute for Space Aeronomy, Brussels, Belgium, [10]Department of Earth and Planetary Science, Graduate School of Frontier Sciences, University of Tokyo, Tokyo, Japan, [11]Faculty of Environmental Earth Science, Hokkaido University, Sapporo, Japan, [12]School of Engineering, University of Shiga Prefecture, Hikone, Japan, [13]British Astronomical Association, London, UK

**Abstract** Even though many missions have explored the Venus atmospheric circulation, its instantaneous state is poorly characterized. In situ measurements vertically sampling the atmosphere exist for limited locations and dates, while remote sensing observations provide only global averages of winds at altitudes of the clouds: 47, 60, and 70 km. We present a three-dimensional global view of Venus's atmospheric circulation from data obtained in June 2007 by the MErcury Surface, Space ENvironment, GEochemistry, and Ranging (MESSENGER) and Venus Express spacecrafts, together with ground-based observations. Winds and temperatures were measured for heights 47–110 km from multiwavelength images and spectra covering 40°N–80°S and local times 12 h–21 h. Dayside westward winds exhibit day-to-day changes, with maximum speeds ranging 97–143 m/s and peaking at variable altitudes within 75–90 km, while on the nightside these peak below cloud tops at ~60 km. Our results support past reports of strong variability of the westward zonal superrotation in the transition region, and good agreement is found above the clouds with results from the Laboratoire de Météorologie Dynamique (LMD) Venus general circulation model.

**Plain Language Summary** The atmosphere of the Earth or Mars globally rotates with a speed similar to the rotation of the planet (approximately 24 h). The rotation of Venus is of about 243 days, much slower than the Earth, but when scientists measured the winds by tracking the clouds of Venus, they discovered that the atmosphere rotates 60 times faster! No one has explained yet what originates this "superrotation," and we do not know well what happens either above or below the clouds. The technique of "Doppler shift" has been used to measure winds above the clouds, but results are "chaotic" and different to interpret. Thanks to a worldwide collaboration in June 2007 between NASA (MESSENGER), ESA (Venus Express), and many observatories (VLT in Chile, JCMT in Hawaii, HHSMT in Arizona, or IRAM in Spain), the authors combined the different data to obtain, for the first time, the instantaneous 3-D structure of the winds on Venus at the clouds and also above, very important for new Venus models to start "forecasts" of the Venus weather with "data assimilation". We also discovered that the superrotation seems unexpectedly different on the night of Venus and that it varies its altitude depending on the day.

## 1. Introduction

The general circulation of the Venus atmosphere consists of two main regimes: a westward superrotating zonal circulation (WSZ, replacing the classical notation RSZ or Retrograde Superrotating Zonal circulation.) which dominates the cloud region from 40 to about 90 km above the surface and a strong subsolar-to-antisolar circulation (SS-AS) above 120 km [see *Schubert et al.*, 2007, Figure 1]. Between them (90–120 km), a complex transition region exists known as upper mesosphere/lower thermosphere [*Lellouch et al.*, 1997;

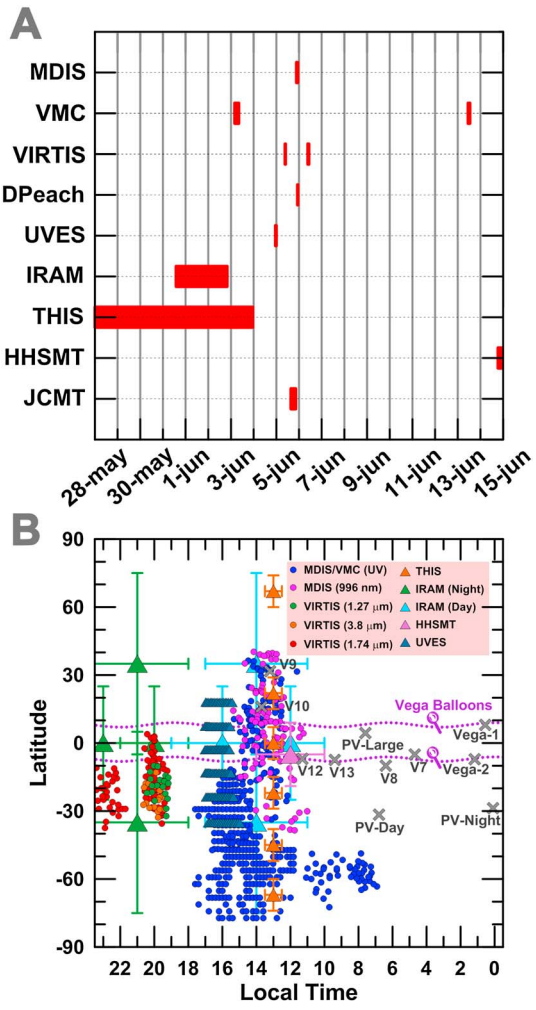


**Figure 1.** (a) Time distribution of the Venus observations coordinated with the MESSG flyby and (b) spatial coverage of our CT wind speeds (circles) and Doppler (triangles). Observations with IRAM and THIS are displayed in Figure 1a without their gaps of observation. In Figure 1b, the smaller bars for HHSMT [*Rengel et al.*, 2008a, Observation 28] compared with IRAM are explained by the technique used by *Rengel et al.* [2008a] and the better instrumental pointing (1" RMS versus 3" RMS) which allowed to overcome the huge size of the HHSMT beam (FWHM of 33"). Every Doppler shift measurement corresponds to a direct estimation of wind, except for the cases of HHSMT [*Rengel et al.*, 2008a] and IRAM [*Lellouch et al.*, 2008] (see Text S1). The entry locations for in situ winds (Veneras, Pioneer Venus and Vega missions) are displayed as grey crosses for comparison.

*Bougher et al.*, 2002]. Different to previous Venus's general circulation models (GCMs) which focused on simulating only the WSZ [*Lee and Richardson*, 2010; *Sugimoto et al.*, 2014] or the SS-AS circulation [*Brecht and Bougher*, 2012; *Bougher et al.*, 2015], new GCMs simulate the bulk atmosphere from the surface to the thermosphere [*Gilli et al.*, 2017] and current efforts are oriented toward "data assimilation" from space missions [*Lahoz et al.*, 2010], which already provided accurate forecasts for the Earth [*Fujita et al.*, 2008; *Yussouf and Stensrud*, 2010] and also Mars [*Rogberg et al.*, 2010; *Hoffman et al.*, 2010]. Thus, acquiring detailed snapshots of the Venus winds at specific moments/epochs is essential to set realistic initial conditions and top/lower boundaries in GCMs with data assimilation. Unfortunately, wind measurements on Venus are dispersed spatially and in time [*Gierasch et al.*, 1997; *Limaye and Rengel*, 2013], and studies analyzing long-term data only focus on the three best known cloud levels [*Peralta et al.*, 2017] and provide time averages, ignoring the time evolution for a given instantaneous 3-D state [*Sánchez-Lavega et al.*, 2008; *Hueso et al.*, 2012, 2015; *Khatuntsev et al.*, 2013; *Kouyama et al.*, 2013]. During the Venus Express (VEx) mission [*Svedhem et al.*, 2007] a coordinated campaign of observations was performed in June 2007 [*Lellouch and Witasse*, 2008], when NASA's spacecraft Mercury Surface, Space Environment, Geochemistry, and Ranging (MESSENGER) (MESSG) made its second flyby of Venus toward Mercury [*McNutt et al.*, 2008]. Despite their potential to reconstruct a 3-D state of the Venusian winds, the results were published as independent works [*Lellouch et al.*, 2008; *Rengel et al.*, 2008a, 2008b; *Clancy et al.*, 2008; *Sornig et al.*, 2008; *Machado et al.*, 2012] while no winds were obtained from the MESSG images [*McNutt et al.*, 2008].

## 2. Observations and Methods

A first realistic approximation to the instantaneous dynamic state of the Venus atmosphere is performed combining new and previously published wind measurements during the flyby, using data from eight instruments of MESSG, VEx, and Earth-based telescopes. The wind speeds and atmospheric temperatures of Venus were calculated for the afternoon and early night during several days around the flyby (see Figure 1) using three remote sensing techniques: Cloud-tracking winds (hereafter, CT) using pairs of images [*Bevington and Robinson*, 1992; *Hueso et al.*, 2010; *Garate-Lopez et al.*, 2013; *Ikegawa and Horinouchi*, 2016] and Doppler and thermal winds derived from the atmospheric spectra and inferred temperatures, respectively [*Piccialli et al.*, 2012]. A summary of the Venus observations used in this work can be found in Table 1 (also Table S1 in the supporting information).

The images for CT were acquired by the cameras MESSG/Mercury Dual Imaging System (MDIS), VEx/Venus Monitoring Camera (VMC), and the imaging spectrometer VEx/Visible and Infrared Thermal Imaging

**Table 1.** Summary of Measurements in This Work

| *Z* (km) | Day/Night | Instrument | Filter/Band | Latitudes | Scale[a](km) of Parameter |
|---|---|---|---|---|---|
| | | | *Winds (Doppler)* | | |
| 110 ± 10 | Day | THIS[b] | 10.4 μm | 67°N–67°S | ~1,500 |
| 85–110 | Day | HHSMT[b] | 220,230 GHz | 13°N–17°S | ~425 |
| 102 ± 8 | Night | IRAM[b] | 230 GHz | 0° | Equatorial wind |
| 94 ± 8 | Both | IRAM[b] | 115,230 GHz | 0° | Equatorial wind |
| 71 ± 3 | Day | UVES[b] | 480–670 nm | 18°N–35°S | ~300 |
| | | | *Winds (Tracking)* | | |
| 98 ± 3 | Night | VEx/VIRTIS-M | 1.27 μm | 10°S–32°S | 190 |
| 71 ± 3 | Day | MESSG/MDIS | 433 nm | 40°N–41°S | 240 |
| 71 ± 3 | Day | VEx/VMC | 365 nm | 12°S–73°S | 370 |
| 71 ± 3 | Day | Amateur | 380–400 nm | 32°N–33°S | ~600 |
| 65 ± 3 | Night | VEx/VIRTIS-M | 3.8 μm | 13°S–33°S | 190 |
| 61 ± 3 | Day | MESSG/MDIS | 996 nm | 40°N–39°S | 200 |
| 50 ± 5 | Night | VEx/VIRTIS-M | 1.74 μm | 03°N–38°S | 190 |
| | | | *Temperature (RTM)* | | |
| 76–116 | Day | JCMT[b] | 330,346 GHz | 80°N–80°S | 5,350 |
| 50–110 | Night | VEx/VIRTIS-M | 4.24–4.54, 4.77–5.01 μm | 13°S–36°S | 18 |

[a]The representative scale of the winds and temperatures are defined in terms of the size of the beam (THIS and JCMT), accuracy of pointing (HHSMT), instant field of view for each CCD cell Ultraviolet and Visual Echelle Spectrograph (UVES), or size of templates used for feature tracking (MDIS,VMC,VIRTIS, and Amateur). IRAM winds are a model-based estimation of the zonal flow at the equator (see Text S1).

[b]Data already published [*Sornig et al.*, 2008; *Rengel et al.*, 2008a; *Lellouch et al.*, 2008; *Machado et al.*, 2012; *Clancy et al.*, 2008], except for part of the data from JCMT.

Spectrometer (VIRTIS-M) [*Hawkins et al.*, 2007; *Markiewicz et al.*, 2007; *Piccioni et al.*, 2007]. These images were taken with different filters to sense the atmospheric motions at several atmospheric levels [*Peralta et al.*, 2017]: the dayside upper clouds at ~60 and ~70 km from the scattered sunlight between 350 and 996 nm [*Hueso et al.*, 2015], the oxygen nightglow (1.27 μm) at 95–100 km [*Hueso et al.*, 2008], the thermal emission of the nocturnal upper clouds (3.8 μm) at ~65 km [*García Muñoz et al.*, 2013], and the night lower clouds' opacity to the deep thermal emission (1.74 μm) at ~50 km [*McGouldrick et al.*, 2008; *Barstow et al.*, 2012]. The vertical uncertainties shown in Table 1 were calculated with radiative transfer models to perform cloud altimetry from several $CO_2$ bands [*Ignatiev et al.*, 2009] and infer the optical depth [*Sánchez-Lavega et al.*, 2008; *Takagi and Iwagami*, 2011; *McGouldrick et al.*, 2008] in the case of scattered sunlight or cloud opacity. The half width at half maximum of the calculated contribution functions was used as reference for $CO_2$ non Local Thermodynamic Equilibrium (non-LTE) [*Lopez-Valverde et al.*, 2016], oxygen airglow [*Lellouch et al.*, 2008; *Gérard et al.*, 2013], and clouds' thermal emissions [*García Muñoz et al.*, 2013]. This vertical uncertainty is later considered in the integration of the thermal wind equation.

Measured atmospheric spectra range from ultraviolet-visible (UV-VIS) wavelengths acquired with the long-slit Echelle-spectrograph VLT/UVES [*Machado et al.*, 2012] to the infrared range covered by VEx/VIRTIS-M and the Cologne Tuneable Heterodyne Infrared Spectrometer (THIS) at the McMath-Pierce Solar Telescope [*Sornig et al.*, 2008] and submillimeter spectra acquired by the Institut de Radio-Astronomie Millimétrique (IRAM) 30 m telescope, the James Clerk Maxwell Telescope (JCMT), and the Heinrich Hertz-Submillimeter Telescope (HHSMT) [*Lellouch et al.*, 2008; *Clancy et al.*, 2008; *Rengel et al.*, 2008a, 2008b]. In contrast with the use of images for CT, the Doppler winds are obtained by means of different instruments and procedures are fully described by the observers [*Sornig et al.*, 2008; *Lellouch et al.*, 2008; *Rengel et al.*, 2008a, 2008b; *Rodgers*, 1976; *Clancy et al.*, 2008; *Machado et al.*, 2012; *Connes*, 1985]. The main characteristics and limitations for these measurements are summarized in Text S1.

Figure 1a displays the time coverage of the observations. Only the UV observations with a small telescope (observer D. Peach) are strictly simultaneous with MDIS, while JCMT and VIRTIS-M performed observations within 24 h around the flyby. Data from the rest of the instruments were acquired several days before and

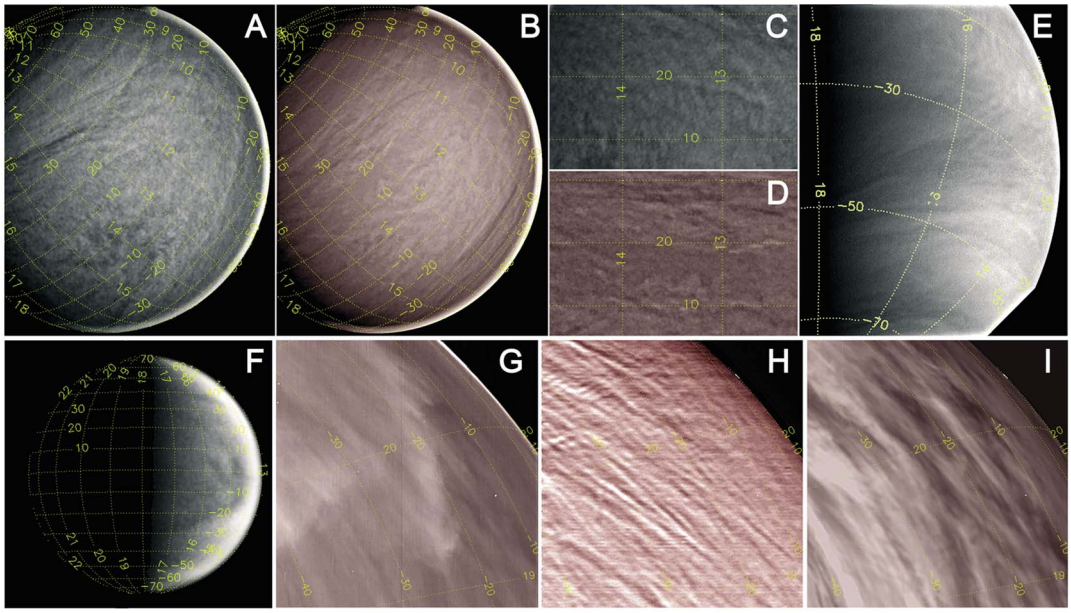


**Figure 2.** Images of Venus taken during the campaign coordinated with the MESSENGER's flyby: (a and b) images taken at 433 nm and 996 nm by MESSG/MDIS; (c and d) cylindrical projections 5°N–30°N in latitude and 240°–280° in longitude from close-up images of MDIS at the same wavelengths (more can be seen in Figure S1); (e) 365 nm image taken with VEx/VMC; (f) a UV image obtained with small telescope by Figure 2d. Peach; finally, (g–i) VEx/VIRTIS-M images taken at 1.27, 3.8, and 1.74 μm. The images were processed to enhance the morphologies.

after the flyby. In the specific case of VMC, the images allowed to extend not only the wind profile to southernmost latitudes but also the time coverage to explore the winds' variability at the cloud tops. The distribution with latitude and local time for our wind speeds (CT and Doppler) is shown in Figure 1b along with the entry locations of in situ measurements with probes [*Gierasch et al.*, 1997; *Crisp et al.*, 1990]. Latitudes between 70°N and 70°S and local times within 12 h–00 h are globally covered. Also, note that although IRAM beams were taken at different locations, only equatorial winds were derived from a global fit of the measurements with a specified latitudinal dependence of the winds [*Lellouch et al.*, 2008] (see Text S1).

Figure 2 shows relevant examples of the Venus images used to obtain CT winds. The mean spatial resolution of the images limits the characteristic scale of our CT winds, shown in Table 1. Due to the fast flyby of MESSG [*McNutt et al.*, 2008], the set of MDIS images analyzed was acquired in only 80 min, with spatial resolutions from ~16 km/pix to 4–3 km/pix. The MDIS images confirm the different cloud morphologies at these two levels of the upper clouds (Figures 2a–2d). Compared to past observations [*Belton et al.*, 1991; *Peralta et al.*, 2007], the near-infrared (NIR) cloud features do not seem anticorrelated with those present in visible (VIS) images (Figures 2a and 2b), and NIR features frequently orientate zonally (see Figures 2c, 2d, and S2) probably due to the weaker meridional circulation at 60 km [*Peralta et al.*, 2007; *Hueso et al.*, 2015]. UV-VIS images during the flyby display an extended dark feature in the afternoon side between the equator and 30°S (see Figures 2a, 2f, and S1), which might be caused by a decrease in the amount of the upper haze and, with a higher degree, by elevated concentrations of the unknown UV absorber [*Titov et al.*, 2008]. Contrasts in the NIR images are mostly caused by the different scattering properties below cloud tops [*Crisp*, 1986; *Takagi and Iwagami*, 2011]. VIRTIS-M images display the variable oxygen airglow at 1.27 μm (Figure 2g) [*Hueso et al.*, 2008], normally more intense at lower latitudes [*Gérard et al.*, 2008]. The upper clouds at 3.8 μm are dominated by narrow bands superimposed to mesoscale wave-like features (Figure 2h), and the lower clouds exhibit variable opacity to the deep thermal emission (Figure 2i).

The atmospheric temperatures of Venus during the flyby are shown in Figure 3. The nightside temperatures (Figure 3a) were calculated for altitudes 50–100 km and 1 km steps using the Radiative Transfer Model developed by *Lee et al.* [2015] and the 4.3 μm $CO_2$ band observable in the spectra from VIRTIS-M cubes and under several assumptions [*Zasova et al.*, 2006; *Grassi et al.*, 2008; *Lee et al.*, 2012] (see Text S1). These temperatures are comparable to the averages from *Grassi et al.* [2014], although during the flyby the atmosphere was slightly colder at lower altitudes. The meridional gradient of temperature is also similar to *Grassi et al.* [2014] within

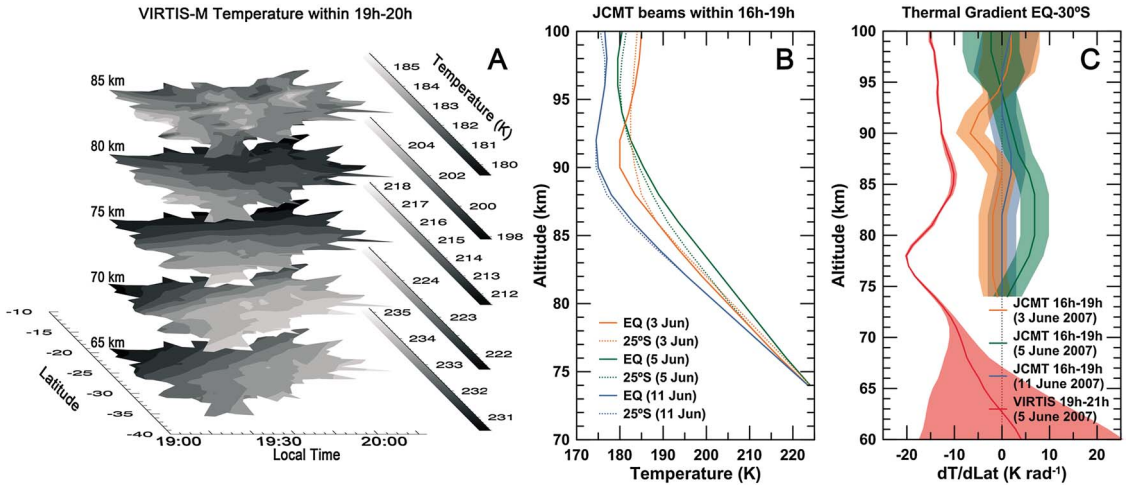


**Figure 3.** Venus's atmospheric temperature during the MESSENGER's flyby: (a) 3-D map of the night temperature derived from the VIRTIS-M spectral cubes used in this work, (b) vertical profiles for the afternoon temperatures obtained with JCMT at different days, and (c) corresponding meridional gradients of temperature between the equator and 30°S.

70–80 km, with temperatures decreasing toward the equator and changing with altitude. The meridional gradient of the dayside temperatures (Figures 3b and 3c) was obtained within a few days of the flyby with ground-based observations of submillimeter $^{12}$CO and $^{13}$CO lines [*Clancy et al.*, 2008]. The meridional gradient at the afternoon seems weaker than in the early night, with temperatures variable in time (scale of days) and increasing toward the equator during the flyby (see Figure 3c).

## 3. Results and Discussion

Doppler, CT, and thermal winds were combined to infer the mean horizontal wind speed at multiple vertical levels of the atmosphere in both day (12 h–17 h) and night (19 h–21 h) of Venus (see Figure 4), toward an approximation to the instantaneous 3-D state of the Venus circulation compared to statistical 3-D views of the cloud layer from VIRTIS-M [*Sánchez-Lavega et al.*, 2008; *Hueso et al.*, 2012] or the dayside upper clouds only [*Khatuntsev et al.*, 2013]. The measurement of the meridional component is constrained to the levels where CT is possible (see Table 1), although this has been recently inferred with the Doppler technique too [*Machado et al.*, 2017]. The meridional profiles in Figures 4a, 4b, 4d, and 4e are similar to the long-term averages during the VEx mission [*Hueso et al.*, 2012, 2015; *Kouyama et al.*, 2013; *Khatuntsev et al.*, 2013], exhibiting the same value of zonal wind between midlatitudes and the equator and a decreasing value from midlatitudes to the poles (Figures 4a and 4d). The meridional component is poleward at the cloud tops (Figure 4b) and usually interpreted as the upper branch of a Hadley-cell circulation [*Limaye*, 2007; *Peralta et al.*, 2007; *Machado et al.*, 2017]. Also in accordance with VEx results, no clear trend is found for the meridional winds at deeper levels of the cloud layer (Figures 4b and 4e). The upper motions of the oxygen nightglow are a complex mixture of westward/eastward and equatorward motions (Figures 4d and 4e) whose statistical distribution is coherent with a SS-AS circulation superimposing the WSZ at this altitude [*Lellouch et al.*, 1994; *Hueso et al.*, 2008; *Soret et al.*, 2014]. Doppler winds at dayside cloud tops (Figure 4a) are ~20 m/s faster than the CT winds from UV-VIS images. The source for this discrepancy, previously reported [*Machado et al.*, 2012, 2014], is unclear yet and might be caused by uncertainties in the vertical level sensed with Doppler in a region with strong shear of the wind (UVES has a wide spectral coverage compared to the narrow filters of MDIS and VMC). Alternatively, Doppler winds might be displaying transient effects like waves [*Machado et al.*, 2017] which are washed out in the CT winds (which involve mean velocities for longer time scales >30 min). Finally, the extremely slow CT motions for the night upper clouds at 65 km (Figure 4d) must not be associated with passive tracers but to the presence of stationary gravity waves similar to the ones identified in Akatsuki/LIR 10- μm images [*Fukuhara et al.*, 2017] which sense the cloud tops level [*Peralta et al.*, 2017].

Since we provide wind measurements at several vertical levels, we now describe the vertical variation of the winds. Toward a coherent comparison with the scale of the meridional gradients of temperature (see Figure 3c), the zonal winds were averaged for the latitude range 0°–30°S and local times 12 h–16 h and 19 h–21 h.

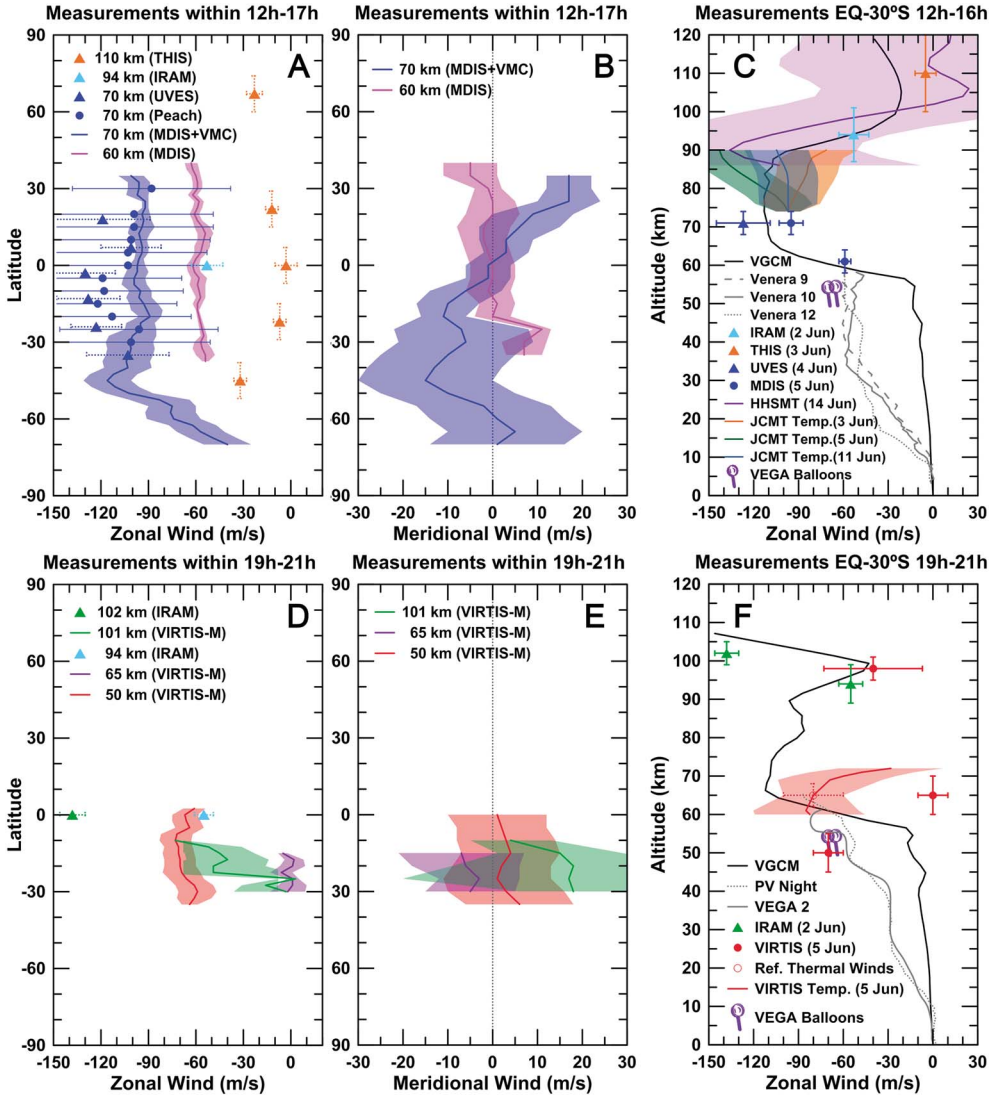


**Figure 4.** Meridional and vertical profiles for the winds of Venus during the MESSG flyby. The zonal and meridional winds are shown for the afternoon of Venus (a and b) 12–17 LT and early night (d and e) 19–21 LT, with wind speeds zonally averaged for these local time ranges. Note that IRAM results for both CO(1-0) (day + night) and CO(2-1) (day) give the same wind value (−60 m/s) at 94 km. Zonal and meridional CT velocities were also averaged in latitude bins of 5° and 10° , respectively. *Error bars/shades* stand for the standard deviation except for THIS, IRAM, and HHSMT (see Text S1). Averaged winds are displayed with continuous lines, except for zonal averages of UVES. (c and f) The vertical profiles of the averaged zonal winds are compared with in situ winds from entry probes, VEGA balloons, and with 12 h–15 h and 18 h–21 h averaged profiles from the GCM by *Gilli et al.* [2017].

Figures 4c and 4f correspond to afternoon during 2–11 June 2007 and early night to 2–5 June. Thermal winds were calculated with the same method as *Newman et al.* [1984, equation (8)]. For the dayside, three dates of JCMT thermal gradients were calculated, while only 1 day of VIRTIS-M observations was obtained for the nightside (Figure 3c). Since we need the winds at a reference level to integrate upward/downward the thermal wind equation, we set for the dayside an average at the cloud top winds ($-95 \pm 8$ m/s), provided that winds at this level kept nearly constant during our observations ($-102 \pm 15$, $-95 \pm 7$, and $-99 \pm 16$ m/s during the days 3, 5, and 13 of June 2007). For the nightside, we chose as reference the upper clouds at ~65 km, using winds of $-80 \pm 20$ m/s averaged from past in situ measurements [*Gierasch et al.*, 1997]. Zonal winds in Figures 4c and 4f are displayed compared with the vertical profiles of zonal wind from the VEGA balloons and probes Veneras 9, 10, and 12, Pioneer Venus Night and VEGA 2, which measured at similar areas of latitude/local time [*Keldysh*, 1977; *Counselman et al.*, 1980; *Moroz and Zasova*, 1997], although the night probes entered the planet outside the local time ranges in this research (see Figure 1b). Zonal winds' profiles predicted by the Venus LMD

GCM [*Gilli et al.*, 2017] are also exhibited. The GCM underestimates winds below 60 km in both day and night. Above this level, the reversed behavior found between day (gradual decrease of the zonal wind toward weak eastward values) and night (decrease followed by a strong recovery up to zonal winds faster than −140 m/s) is predicted by the GCM. Similar range of wind speeds is usually found with Doppler winds [*Limaye and Rengel*, 2013] as part of the strong variability reported for the WSZ at these altitudes [*Bougher et al.*, 1997]. The rapid increase in the westward winds within 19 h–21 h above 100 km (Figure 4f) seems justified in the GCM by the presence of a strong thermal gradient [*Gilli et al.*, 2017, Figure 8]. The GCM does not predict the step decrease in the night thermal winds at the upper clouds (Figure 4f), apparently related to a sudden breakdown of the cyclostrophic balance from ∼73 km.

Despite the poor sampling of temperatures with JCMT and associated errors, a succinct analysis of the time variability in the thermal winds was performed. Our results show that both the height and maximum value of the zonal wind peak seem subject to significant changes on the dayside, with altitudes ±15 km about the cloud tops and speeds ranging from −97 ± 8 m/s to −143 ± 21 m/s (see Figure S2). The timescale for these variations is of about several Earth days and seem associated with the fast changes on the dayside temperatures, also reported in previous works [*Clancy et al.*, 2003]. Changes with similar timescales have been repeatedly reported on Doppler winds [*Clancy et al.*, 2008, 2012]. As a result, the WSZ circulation seems to vary its vertical dominion, being shifted to deeper heights with atmospheric density up to 2 orders of magnitude higher, which is also consistent with a lower value for the maximum wind speed (Figure 4c). Regarding the nightside (5 June, Figure 4f), the zonal wind peaks even deeper (∼60 km) with speeds ∼ −90 m/s, weaker than on dayside. This behavior is also consistent with the interpretation of eventual vertical invasions of the SS-AS circulation down to deeper altitudes [*Lellouch et al.*, 1997; *Widemann et al.*, 2007; *Sornig et al.*, 2008; *Limaye and Rengel*, 2013].

## 4. Conclusions

The combination of coordinated ground-based observations with space missions is demonstrated to be a powerful tool to characterize the instantaneous state of planetary atmospheres and can stimulate new campaigns with professional/amateur astronomers [*Sánchez-Lavega et al.*, 2016] during the ongoing JAXA's Akatsuki mission [*Nakamura et al.*, 2016; *Peralta et al.*, 2017]. Combining three techniques to measure winds and data from nine instruments, we derived — for the first time — vertical profiles of the zonal wind using only remote sensing data and extending from the clouds up to the transition region. The vertical behavior of the zonal wind importantly varies with time and from day to night, supporting a vertical variability for the vertical dominion of the WSZ circulation, maybe caused by an eventual vertical invasion of the SS-AS circulation. Finally, GCMs with *data assimilation* [*Navarro et al.*, 2016] will be able to test the time evolution shown for the 3-D winds on the dayside.

**Acknowledgments**

J.P. acknowledges JAXA's International Top Young Fellowship. R.H. and A.S.-L. were supported by the Spanish project AYA2015-65041-P (MINECO/FEDER, UE), Grupos Gobierno Vasco IT-765-13 and Universidad del País Vasco UPV/EHU program UFI11/55. A.P. acknowledges support from the FP-7 project EUROVENUS of the European Union. We thank *S. Lebonnois* and *G. Gilli* for providing the vertical profiles predicted by the LMD Venus GCM. We are also grateful to the anonymous reviewers for their useful comments to improve the manuscript. All the images used in this work can be downloaded from the public URLs included in the supporting information; any additional data may be obtained from the authors.

## References

Barstow, J. K., C. C. C. Tsang, C. F. Wilson, P. G. J. Irwin, F. W. Taylor, K. McGouldrick, P. Drossart, G. Piccioni, and S. Tellmann (2012), Models of the global cloud structure on Venus derived from Venus Express observations, *Icarus*, *217*, 542–560, doi:10.1016/j.icarus.2011.05.018.

Belton, M. J. S., P. J. Gierasch, M. D. Smith, P. Helfenstein, P. J. Schinder, J. B. Pollack, K. A. Rages, D. Morrison, K. P. Klaasen, and C. B. Pilcher (1991), Images from Galileo of the Venus cloud deck, *Science*, *253*, 1531–1536.

Bevington, P. R., and D. K. Robinson (1992), *Data Reduction and Error Analysis for the Physical Sciences*, 2nd ed., McGraw-Hill, New York.

Bougher, S. W., M. J. Alexander, and H. G. Mayr (1997), Upper atmosphere dynamics: Global circulation and gravity waves, in *Venus II: Geology, Geophysics, Atmosphere, and Solar Wind Environment*, edited by S. W. Bougher, D. M. Hunten, and R. J. Phillips, pp. 259–291, Univ. of Arizona Press, Tucson, Ariz.

Bougher, S. W., R. G. Roble, and T. Fuller-Rowell (2002), Simulations of the upper atmospheres of the terrestrial planets, in *Atmospheres in the Solar System: Comparative Aeronomy. Geophys. Monogr.*, vol. 130, p. 261, AGU, Washington, D. C.

Bougher, S. W., A. S. Brecht, R. Schulte, J. Fischer, C. D. Parkinson, A. Mahieux, V. Wilquet, and A. Vandaele (2015), Upper atmosphere temperature structure at the Venusian terminators: A comparison of SOIR and VTGCM results, *Planet. Space Sci.*, *113*, 336–346, doi:10.1016/j.pss.2015.01.012.

Brecht, A. S., and S. W. Bougher (2012), Dayside thermal structure of Venus' upper atmosphere characterized by a global model, *J. Geophys. Res.*, *117*, E08002, doi:10.1029/2012JE004079.

Clancy, R. T., B. J. Sandor, and G. H. Moriarty-Schieven (2003), Observational definition of the Venus mesopause: Vertical structure, diurnal variation, and temporal instability, *Icarus*, *161*, 1–16, doi:10.1016/S0019-1035(02)00022-2.

Clancy, R. T., B. J. Sandor, and G. H. Moriarty-Schieven (2008), Venus upper atmospheric CO, temperature, and winds across the afternoon/evening terminator from June 2007 JCMT sub-millimeter line observations, *Planet. Space Sci.*, *56*, 1344–1354, doi:10.1016/j.pss.2008.05.007.

Clancy, R. T., B. J. Sandor, and G. Moriarty-Schieven (2012), Circulation of the Venus upper mesosphere/lower thermosphere: Doppler wind measurements from 2001-2009 inferior conjunction, sub-millimeter CO absorption line observations, *Icarus*, *217*, 794–812, doi:10.1016/j.icarus.2011.05.021.

Connes, P. (1985), Absolute astronomical accelerometry, *Astrophys. Space Sci.*, *110*, 211–255, doi:10.1007/BF00653671.
Counselman, C. C., S. A. Gourevitch, R. W. King, G. B. Loriot, and E. S. Ginsberg (1980), Zonal and meridional circulation of the lower atmosphere of Venus determined by radio interferometry, *J. Geophys. Res.*, *85*, 8026–8030.
Crisp, D. (1986), Radiative forcing of the Venus mesosphere. I—Solar fluxes and heating rates, *Icarus*, *67*, 484–514, doi:10.1016/0019-1035(86)90126-0.
Crisp, D., A. P. Ingersoll, C. E. Hildebrand, and R. A. Preston (1990), VEGA balloon meteorological measurements, *Adv. Space Res.*, *10*, 109–124, doi:10.1016/0273-1177(90)90172-V.
Fujita, T., D. J. Stensrud, and D. C. Dowell (2008), Using precipitation observations in a mesoscale short-range ensemble analysis and forecasting system, *Weather Forecasting*, *23*, 357, doi:10.1175/2007WAF2006108.1.
Fukuhara, T., et al. (2017), Large stationary gravity wave in the atmosphere of Venus, *Nat. Geosci.*, doi:10.1038/ngeo2873.
Garate-Lopez, I., R. Hueso, A. Sánchez-Lavega, J. Peralta, G. Piccioni, and P. Drossart (2013), A chaotic long-lived vortex at the southern pole of Venus, *Nat. Geosci.*, *6*, 254–257, doi:10.1038/ngeo1764.
García Muñoz, A., P. Wolkenberg, A. Sánchez-Lavega, R. Hueso, and I. Garate-Lopez (2013), A model of scattered thermal radiation for Venus from 3 to 5$\mu$m, *Planet. Space Sci.*, *81*, 65–73, doi:10.1016/j.pss.2013.03.007.
Gérard, J.-C., A. Saglam, G. Piccioni, P. Drossart, C. Cox, S. Erard, R. Hueso, and A. Sánchez-Lavega (2008), Distribution of the $O_2$ infrared nightglow observed with VIRTIS on board Venus Express, *Geophys. Res. Lett.*, *35*, L02207, doi:10.1029/2007GL032021.
Gérard, J.-C., L. Soret, A. Migliorini, and G. Piccioni (2013), Oxygen nightglow emissions of Venus: Vertical distribution and collisional quenching, *Icarus*, *223*, 602–608, doi:10.1016/j.icarus.2012.11.019.
Gierasch, P. J., et al. (1997), The general circulation of the Venus atmosphere: An assessment, in *Venus II — Geology, Geophysics, Atmosphere, and Solar Wind Environment*, pp. 459–500, Univ. of Arizona Press, Tucson, Ariz.
Gilli, G., S. Lebonnois, F. González-Galindo, M. A. López-Valverde, A. Stolzenbach, F. Lefévre, J. Y. Chaufray, and F. Lott (2017), Thermal structure of the upper atmosphere of Venus simulated by a ground-to-thermosphere {GCM}, *Icarus*, *281*, 55–72, doi:10.1016/j.icarus.2016.09.016.
Grassi, D., P. Drossart, G. Piccioni, N. I. Ignatiev, L. V. Zasova, A. Adriani, M. L. Moriconi, P. G. J. Irwin, A. Negrão, and A. Migliorini (2008), Retrieval of air temperature profiles in the Venusian mesosphere from VIRTIS-M data: Description and validation of algorithms, *J. Geophys. Res.*, *113*, E00B09, doi:10.1029/2008JE003075.
Grassi, D., R. Politi, N. I. Ignatiev, C. Plainaki, S. Lebonnois, P. Wolkenberg, L. Montabone, A. Migliorini, G. Piccioni, and P. Drossart (2014), The Venus nighttime atmosphere as observed by the VIRTIS-M instrument. Average fields from the complete infrared data set, *J. Geophys. Res. Planets*, *119*, 837–849, doi:10.1002/2013JE004586.
Hawkins, S. E., et al. (2007), The Mercury dual imaging system on the MESSENGER spacecraft, *Space Sci. Rev.*, *131*, 247–338, doi:10.1007/s11214-007-9266-3.
Hoffman, M. J., S. J. Greybush, R. John Wilson, G. Gyarmati, R. N. Hoffman, E. Kalnay, K. Ide, E. J. Kostelich, T. Miyoshi, and I. Szunyogh (2010), An ensemble Kalman filter data assimilation system for the martian atmosphere: Implementation and simulation experiments, *Icarus*, *209*, 470–481, doi:10.1016/j.icarus.2010.03.034.
Hueso, R., A. Sánchez-Lavega, G. Piccioni, P. Drossart, J. C. Gérard, I. Khatuntsev, L. Zasova, and A. Migliorini (2008), Morphology and dynamics of Venus oxygen airglow from Venus Express/Visible and Infrared Thermal Imaging Spectrometer observations, *J. Geophys. Res.*, *113*, E00B02, doi:10.1029/2008JE003081.
Hueso, R., J. Legarreta, J. F. Rojas, J. Peralta, S. Pérez-Hoyos, T. del Río-Gaztelurrutia, and A. Sánchez-Lavega (2010), The Planetary Laboratory for Image Analysis (PLIA), *Adv. Space Res.*, *46*, 1120–1138, doi:10.1016/j.asr.2010.05.016.
Hueso, R., J. Peralta, and A. Sánchez-Lavega (2012), Assessing the long-term variability of Venus winds at cloud level from VIRTIS-Venus Express, *Icarus*, *217*, 585–598, doi:10.1016/j.icarus.2011.04.020.
Hueso, R., J. Peralta, I. Garate-Lopez, T. V. Bandos, and A. Sánchez-Lavega (2015), Six years of Venus winds at the upper cloud level from UV, visible and near infrared observations from VIRTIS on Venus Express, *Planet. Space Sci.*, *113*, 78–99, doi:10.1016/j.pss.2014.12.010.
Ignatiev, N. I., D. V. Titov, G. Piccioni, P. Drossart, W. J. Markiewicz, V. Cottini, T. Roatsch, M. Almeida, and N. Manoel (2009), Altimetry of the Venus cloud tops from the Venus Express observations, *J. Geophys. Res.*, *114*, E00B43, doi:10.1029/2008JE003320.
Ikegawa, S., and T. Horinouchi (2016), Improved automatic estimation of winds at the cloud top of Venus using superposition of cross-correlation surfaces, *Icarus*, *271*, 98–119, doi:10.1016/j.icarus.2016.01.018.
Keldysh, M. V. (1977), Venus exploration with the Venera 9 and Venera 10 spacecraft, *Icarus*, *30*, 605–625, doi:10.1016/0019-1035(77)90085-9.
Khatuntsev, I. V., M. V. Patsaeva, D. V. Titov, N. I. Ignatiev, A. V. Turin, S. S. Limaye, W. J. Markiewicz, M. Almeida, T. Roatsch, and R. Moissl (2013), Cloud level winds from the Venus Express Monitoring Camera imaging, *Icarus*, *226*, 140–158, doi:10.1016/j.icarus.2013.05.018.
Kouyama, T., T. Imamura, M. Nakamura, T. Satoh, and Y. Futaana (2013), Long-term variation in the cloud-tracked zonal velocities at the cloud top of Venus deduced from Venus Express VMC images, *J. Geophys. Res. Planets*, *118*, 37–46, doi:10.1029/2011JE004013.
Lahoz, W., B. Khattatov, and R. Menard (2010), *Data Assimilation: Making Sense of Observations*, Springer, Berlin.
Lee, C., and M. I. Richardson (2010), A general circulation model ensemble study of the atmospheric circulation of Venus, *J. Geophys. Res.*, *115*, E04002, doi:10.1029/2009JE003490.
Lee, Y. J., D. V. Titov, S. Tellmann, A. Piccialli, N. Ignatiev, M. Pätzold, B. Häusler, G. Piccioni, and P. Drossart (2012), Vertical structure of the Venus cloud top from the VeRa and VIRTIS observations onboard Venus Express, *Icarus*, *217*, 599–609, doi:10.1016/j.icarus.2011.07.001.
Lee, Y. J., D. V. Titov, N. I. Ignatiev, S. Tellmann, M. Pätzold, and G. Piccioni (2015), The radiative forcing variability caused by the changes of the upper cloud vertical structure in the Venus mesosphere, *Planet. Space Sci.*, *113*, 298–308, doi:10.1016/j.pss.2014.12.006.
Lellouch, E., and O. Witasse (2008), A coordinated campaign of Venus ground-based observations and Venus Express measurements, *Planet. Space Sci.*, *56*, 1317–1319, doi:10.1016/j.pss.2008.07.001.
Lellouch, E., J. J. Goldstein, J. Rosenqvist, S. W. Bougher, and G. Paubert (1994), Global circulation, thermal structure, and carbon monoxide distribution in Venus' mesosphere in 1991, *Icarus*, *110*, 315–339, doi:10.1006/icar.1994.1125.
Lellouch, E., T. Clancy, D. Crisp, A. J. Kliore, D. Titov, and S. W. Bougher (1997), Monitoring of mesospheric structure and dynamics, in *Venus II: Geology, Geophysics, Atmosphere, and Solar Wind Environment*, edited by S. W. Bougher, D. M. Hunten, and R. J. Phillips, p. 295, Univ. of Arizona Press, Tucson, Ariz.
Lellouch, E., G. Paubert, R. Moreno, and A. Moullet (2008), Monitoring Venus' mesospheric winds in support of Venus Express: IRAM 30-m and APEX observations, *Planet. Space Sci.*, *56*, 1355–1367.
Limaye, S. S. (2007), Venus atmospheric circulation: Known and unknown, *J. Geophys. Res.*, *112*, E04S09, doi:10.1029/2006JE002814.
Limaye, S. S., and M. Rengel (2013), Atmospheric circulation and dynamics, in *Towards Understanding the Climate of Venus*, pp. 55–70, Springer, New York, doi:10.1007/978-1-4614-5064-1_5.

Lopez-Valverde, M. A., L. Montabone, M. Sornig, and G. Sonnabend (2016), On the retrieval of mesospheric winds on Mars and Venus from ground-based observations at 10 $\mu$m, *Astrophys. J.*, *816*, 103, doi:10.3847/0004-637X/816/2/103.

Machado, P., D. Luz, T. Widemann, E. Lellouch, and O. Witasse (2012), Mapping zonal winds at Venus's cloud tops from ground-based Doppler velocimetry, *Icarus*, *221*, 248–261, doi:10.1016/j.icarus.2012.07.012.

Machado, P., T. Widemann, D. Luz, and J. Peralta (2014), Wind circulation regimes at Venus' cloud tops: Ground-based Doppler velocimetry using CFHT/ESPaDOnS and comparison with simultaneous cloud tracking measurements using VEx/VIRTIS in February 2011, *Icarus*, *243*, 249–263, doi:10.1016/j.icarus.2014.08.030.

Machado, P., T. Widemann, J. Peralta, R. Gonçalves, J.-F. Donati, and D. Luz (2017), Venus cloud-tracked and doppler velocimetry winds from CFHT/ESPaDOnS and Venus Express/VIRTIS in April 2014, *Icarus*, *285*, 8–26, doi:10.1016/j.icarus.2016.12.017.

Markiewicz, W. J., et al. (2007), Venus monitoring camera for Venus express, *Planet. Space Sci.*, *55*, 1701–1711, doi:10.1016/j.pss.2007.01.004.

McGouldrick, K., K. H. Baines, T. W. Momary, and D. H. Grinspoon (2008), Venus Express/VIRTIS observations of middle and lower cloud variability and implications for dynamics, *J. Geophys. Res.*, *113*, E00B14, doi:10.1029/2008JE003113.

McNutt, R. L., Jr., S. C. Solomon, D. G. Grant, E. J. Finnegan, and P. D. Bedini (2008), The MESSENGER mission to Mercury: Status after the Venus flybys, *Acta Astronaut.*, *63*, 68–73.

Moroz, V. I., and L. V. Zasova (1997), VIRA-2: A review of inputs for updating the Venus International Reference Atmosphere, *Adv. Space Res.*, *19*, 1191–1201, doi:10.1016/S0273-1177(97)00270-6.

Nakamura, M., et al. (2016), AKATSUKI returns to Venus, *Earth Planets Space*, *68*(1), 1–10, doi:10.1186/s40623-016-0457-6.

Navarro, T., F. Forget, and E. Millour (2016), *Using Data Assimilation to Compare Models of Mars and Venus Atmospheres With Observations*, vol. 210.07, AAS/Division for Planetary Sciences Meeting.

Newman, M., G. Schubert, A. J. Kliore, and I. R. Patel (1984), Zonal winds in the middle atmosphere of Venus from Pioneer Venus radio occultation data, *J. Atmos. Sci.*, *41*, 1901–1913.

Peralta, J., R. Hueso, and A. Sánchez-Lavega (2007), A reanalysis of Venus winds at two cloud levels from Galileo SSI images, *Icarus*, *190*, 469–477, doi:10.1016/j.icarus.2007.03.028.

Peralta, J., Y. J. Lee, K. McGouldrick, H. Sagawa, A. Sánchez-Lavega, T. Imamura, T. Widemann, and M. Nakamura (2017), Overview of useful spectral regions for Venus: An update to encourage observations complementary to the Akatsuki mission, *Icarus*, *288*, 235–239, doi:10.1016/j.icarus.2017.01.027.

Piccialli, A., S. Tellmann, D. V. Titov, S. S. Limaye, I. V. Khatuntsev, M. Pätzold, and B. Häusler (2012), Dynamical properties of the Venus mesosphere from the radio-occultation experiment VeRa onboard Venus Express, *Icarus*, *217*, 669–681, doi:10.1016/j.icarus.2011.07.016.

Piccioni, G., et al. (Eds.) (2007), *VIRTIS: The Visible and Infrared Thermal Imaging Spectrometer*, vol. 1295, ESA Special Publ.

Rengel, M., P. Hartogh, and C. Jarchow (2008a), Mesospheric vertical thermal structure and winds on Venus from HHSMT CO spectral-line observations, *Planet. Space Sci.*, *56*, 1368–1384, doi:10.1016/j.pss.2008.07.004.

Rengel, M., P. Hartogh, and C. Jarchow (2008b), HHSMT observations of the Venusian mesospheric temperature, winds, and CO abundance around the MESSENGER flyby, *Planet. Space Sci.*, *56*, 1688–1695, doi:10.1016/j.pss.2008.07.014.

Rodgers, C. D. (1976), Retrieval of atmospheric temperature and composition from remote measurements of thermal radiation, *Rev. Geophys.*, *14*, 609–624, doi:10.1029/RG014i004p00609.

Rogberg, P., P. L. Read, S. R. Lewis, and L. Montabone (2010), Assessing atmospheric predictability on Mars using numerical weather prediction and data assimilation, *Q. J. R. Meteorol. Soc.*, *136*, 1614–1635, doi:10.1002/qj.677.

Sánchez-Lavega, A., et al. (2008), Variable winds on Venus mapped in three dimensions, *Geophys. Res. Lett.*, *35*, L13204, doi:10.1029/2008GL033817.

Sánchez-Lavega, A., J. Peralta, J. M. Gomez-Forrellad, R. Hueso, S. Pérez-Hoyos, I. Mendikoa, J. F. Rojas, T. Horinouchi, Y. J. Lee, and S. Watanabe (2016), Venus cloud morphology and motions from ground-based images at the time of the Akatsuki orbit insertion, *Astrophys. J. Lett.*, *833*, L7, doi:10.3847/2041-8205/833/1/L7.

Schubert, G., S. W. Bougher, C. C. Covey, A. D. Del Genio, A. S. Grossman, J. L. Hollingsworth, S. S. Limaye, and R. E. Young (2007), Venus atmosphere dynamics: A continuing enigma, in *Exploring Venus as a Terrestrial Planet, Geophys. Monogr. Ser.*, vol. 176, pp. 101–120, AGU, Washington, D. C., doi:10.1029/176GM07.

Soret, L., J.-C. Gérard, G. Piccioni, and P. Drossart (2014), Time variations of $O_2(a^1\Delta)$ nightglow spots on the Venus nightside and dynamics of the upper mesosphere, *Icarus*, *237*, 306–314, doi:10.1016/j.icarus.2014.03.034.

Sornig, M., T. Livengood, G. Sonnabend, P. Kroetz, D. Stupar, T. Kostiuk, and R. Schieder (2008), Venus upper atmosphere winds from ground-based heterodyne spectroscopy of $CO_2$ at 10$\mu$m wavelength, *Planet. Space Sci.*, *56*, 1399–1406, doi:10.1016/j.pss.2008.05.006.

Sugimoto, N., M. Takagi, and Y. Matsuda (2014), Waves in a Venus general circulation model, *Geophys. Res. Lett.*, *41*, 7461–7467, doi:10.1002/2014GL061807.

Svedhem, H., et al. (2007), Venus express: The first European mission to Venus, *Planet. Space Sci.*, *55*, 1636–1652, doi:10.1016/j.pss.2007.01.013.

Takagi, S., and N. Iwagami (2011), Contrast sources for the infrared images taken by the Venus mission AKATSUKI, *Earth Planets Space*, *63*, 435–442, doi:10.5047/eps.2011.01.007.

Titov, D. V., F. W. Taylor, H. Svedhem, N. I. Ignatiev, W. J. Markiewicz, G. Piccioni, and P. Drossart (2008), Atmospheric structure and dynamics as the cause of ultraviolet markings in the clouds of Venus, *Nature*, *456*, 620–623, doi:10.1038/nature07466.

Widemann, T., E. Lellouch, and A. Campargue (2007), New wind measurements in Venus' lower mesosphere from visible spectroscopy, *Planet. Space Sci.*, *55*, 1741–1756, doi:10.1016/j.pss.2007.01.005.

Yussouf, N., and D. J. Stensrud (2010), Impact of phased-array radar observations over a short assimilation period: Observing system simulation experiments using an ensemble Kalman filter, *Mon. Weather Rev.*, *138*, 517, doi:10.1175/2009MWR2925.1.

Zasova, L. V., V. I. Moroz, V. M. Linkin, I. V. Khatuntsev, and B. S. Maiorov (2006), Structure of the Venusian atmosphere from surface up to 100 km, *Cosmic Res.*, *44*, 364–383, doi:10.1134/S0010952506040095.